



**Comparative Toxicity Assessment of Novel Si Quantum Dots
and their Traditional Cd-based Counterparts using Bacteria
Models *Shewanella oneidensis* and *Bacillus subtilis***

Journal:	<i>Environmental Science: Nano</i>
Manuscript ID	EN-ART-03-2018-000332.R1
Article Type:	Paper
Date Submitted by the Author:	18-Jun-2018
Complete List of Authors:	Pramanik, Sunipa; University of Minnesota Hill, Samantha; University of Minnesota Zhi, Bo; University of Minnesota, Chemistry Hudson-Smith, Natalie; University of Minnesota Wu, Jeslin; University of Minnesota White, Jacob; University of Minnesota McIntire, Eileen; University of Minnesota Kondeti, Vighneswara; University of Minnesota Lee, Amani; University of Minnesota Bruggeman, Peter; University of Minnesota Kortshagen, Uwe; University of Minnesota, Haynes, Christy; University of Minnesota,

1
2
3 **Comparative Toxicity Assessment of Novel Si Quantum Dots and their Traditional Cd-**
4 **based Counterparts using Bacteria Models *Shewanella oneidensis* and *Bacillus subtilis***
5
6
7

8 Sunipa Pramanik,^a Samantha K. E. Hill,^b Bo Zhi,^a Natalie V. Hudson-Smith,^a Jeslin J. Wu,^b
9
10 Jacob N. White,^a Eileen A. McIntire,^a V. S. Santosh K. Kondeti,^b Amani L. Lee,^a Peter J.
11
12 Bruggeman,^b Uwe R. Kortshagen,^b Christy L. Haynes^{a*}
13
14
15

16 ^aDepartment of Chemistry, University of Minnesota, 207 Pleasant St SE, Minneapolis, MN
17
18 55455, USA
19
20

21 ^bDepartment of Mechanical Engineering, University of Minnesota, 111 Church St SE,
22
23 Minneapolis 55455, USA
24
25

26 *corresponding author: chaynes@umn.edu
27
28

29 **Abstract:** Quantum dots are crystalline semiconductor nanoparticles with unique optical
30
31 properties due to quantum confinement effects. They have several advantages compared to
32
33 traditional organic fluorescent dyes, such as high fluorescent brightness, photostability, and
34
35 tunable emission wavelengths, dependent upon particle size. Their unique optical properties have
36
37 led to an increased use in a variety of devices, including diode lasers and television displays, as
38
39 well as in biomedical research. The most commonly used quantum dots (QDs) are made of
40
41 cadmium selenide (CdSe) and have cadmium selenide core with zinc sulfide shell (CdSe/ZnS),
42
43 containing inherently toxic cadmium. This work focuses on comparison of the toxic effects of
44
45 conventional CdSe and CdSe/ZnS quantum dots and silicon quantum dots, which are emerging
46
47 as a potentially benign alternative, using bacteria as a model organism. The bacteria models used
48
49 for our studies are *Shewanella oneidensis* MR-1, a Gram-negative bacterium, and *Bacillus*
50
51 *subtilis* SB 491, a Gram-positive bacterium. This research assesses changes in cell viability,
52
53
54
55
56
57
58
59
60

1
2
3 respiration pattern, and cell membrane integrity in the presence of the nanoparticles using colony
4 counting, respirometry and membrane integrity assays, respectively. The association of the QDs
5 with bacterial cell membranes was investigated using transmission electron microscopy (TEM).
6 Results indicate that the silicon QDs are benign to the bacteria considered, and they do not
7 associate with the cell membranes. The CdSe cores exhibit significant toxicity to the bacterial
8 cells, whereas the CdSe/ZnS QDs are comparatively less toxic.
9

10
11
12
13
14
15
16
17 **Environmental significance statement:** QDs are presently used in electronic displays because
18 of their electronic and optical properties that can improve the color gamut and brightness, and
19 even reduce power consumption. Cd-based QDs have been primarily used for these applications
20 based on their high quantum efficiencies. However, the presence of toxic cadmium metal in these
21 QDs makes them a potential risk to the environment as their use increases and products reach
22 end of life. The work herein focuses on a silicon-based alternative QD and compares the
23 interactions between the different kinds of QDs (silicon and Cd-based) and bacterial cells. The
24 interaction of QDs with environmentally beneficial bacteria are an indicator of how these QDs
25 may behave once released into the environment. Because the silicon-based QDs are less toxic to
26 the bacterial cells than the Cd-based QDs, as well as made of an earth-abundant element, the
27 silicon-based QDs offer a sustainable and environmentally friendly alternative to Cd-based QDs
28 for commercial products. The Cd-based QDs have been preferred in commercial products due to
29 their superior performance and luminescence properties. Even though the Si-based QDs have
30 high quantum yields, further scientific research is ongoing to improve their properties so they
31 can fulfill their potential as an alternative option not only from a sustainability point of view, but
32 also from a performance point of view.
33
34
35
36
37
38
39
40
41
42
43
44
45
46
47
48
49
50
51
52
53

54
55 **Introduction:**
56
57
58
59
60

1
2
3 An enormous growth in the use of nanotechnology-based products in the last ten years means
4 that there is an increased risk of human and environmental exposure to engineered
5 nanomaterials. It is thus important to investigate the behavior of industrially relevant engineered
6 nanomaterials in the environment, as well as their toxicity towards living organisms. Based on
7 their unique electronic and optical properties, there has been considerable interest in the
8 synthesis and application of semiconductor nanocrystals in recent years.^{1 3} Quantum dots (QDs)
9 are crystalline semiconducting nanomaterials that display quantum confinement effects, a
10 property exhibited by nanocrystals smaller in size than the Bohr radius, and have been
11 traditionally synthesized from toxic and rare metals, such as cadmium.^{2,3} The result is a size-
12 dependent band gap and thus, extraordinary optical properties.^{4,5} QDs were first discovered
13 entrapped in a silicate glass matrix by A. I. Ekimov and A. A. Onushchenko in 1981⁶ and have
14 since become the subject of intensive research⁷⁻¹⁶ based on their advantages over traditional
15 organic fluorescent dyes, such as high luminescent brightness, good photostability, and tunable
16 size-dependent emission wavelengths. The unique optical properties of QDs have led to their
17 increased use in a variety of devices, including light-emitting diodes for electronic displays as
18 well as in biomedical research. The total market impact of QDs is projected to reach around \$3.4
19 billion by 2021, with the electronics sector totaling around \$1.1 billion and the optoelectronics
20 sector just over \$1.8 billion, according to a study done by BCC Research titled “Quantum Dots:
21 Global Market Growth and Future Commercial Prospects,” published in September 2016.
22 Leading electronic companies such as Philips and Samsung have QD-based LCD displays in
23 their devices currently on the market.¹⁷

24
25
26
27
28
29
30
31
32
33
34
35
36
37
38
39
40
41
42
43
44
45
46
47
48
49
50
51
52
53
54
55
56
57
58
59
60
The increasing use of QDs in commercial products has led to concerns regarding their
environmental impact. 41.8 million tons of e-waste was generated in 2014 globally, of which

1
2
3 only 6.5 million tons were collected and treated by respective national electronic take-back
4 systems.¹⁸ Only 12% of the e-waste generated in United States and Canada is collected by
5 designated organizations and sent to facilities to remove toxic materials before being disposed of
6 in landfills or incinerators. A majority of the e-waste that is discarded as regular mixed waste
7 directly ends up in landfills without any prior treatment and can be hazardous to the
8 environment. Although there has been extensive research about the toxicity of QDs to
9 mammalian cells as a model for potential implications on human health,^{19,20} the effect of
10 quantum dots on the various trophic levels of the ecosystem are not as well characterized.
11 Previous studies have identified the leaching of toxic ions, such as Cd, from QDs and generation
12 of reactive oxygen species (ROS) as the main contributing factors to QD toxicity.^{21,22,23} CdTe
13 QDs have been reported to inflict oxidative damage on *Escherichia coli* cells.²⁴ Growth
14 inhibition and lipid peroxidation have been observed in the microalgae *Phaeodactylum*
15 *tricornutum* in the presence of CdSe/ZnS QDs due to ROS generation.²⁵ Biomagnification and
16 accumulation of QDs have also been observed in certain freshwater and seawater species.²⁶ As
17 the dissolution to Cd ions is one of the major pathways of quantum dot toxicity, some
18 researchers have been focusing on the synthesis of Cd-free quantum dots or the inclusion of
19 other design elements that block Cd release.²⁷ For example, the incorporation of a ZnS shell
20 around the Cd-based core is a common strategy used to mitigate QD toxicity.
21
22
23
24
25
26
27
28
29
30
31
32
33
34
35
36
37
38
39
40
41
42
43
44
45
46

47 This work focuses on Cd-free quantum dots using the earth-abundant and potentially more
48 benign element silicon to make silicon quantum dots (SiQDs) and presents a detailed comparison
49 of the optical properties and environmental toxicity of the SiQDs to the more traditional CdSe
50 and CdSe/ZnS QDs. The luminescent SiQDs used in this study were synthesized in a low-
51
52
53
54
55
56
57
58
59
60

1
2
3 pressure, non-thermal plasma and subsequently treated with an atmospheric pressure
4 microplasma to make them dispersible in water due to formation of a silica shell.²⁸ SiQDs tend to
5 exhibit broad luminescence peaks, unlike more conventionally used QDs. Most of the
6 semiconducting materials used to make QDs are direct band gap materials, whereas Si is an
7 indirect band gap materials, thus leading to its unusual optical profiles.²⁹ There are mixed
8 outcomes within the limited examples investigating the nanotoxicity of silicon-based QDs in the
9 literature. SiQDs have been shown to induce inflammation in MRC-5 human lung fibroblasts by
10 causing cell membrane damage, affecting the actin filaments, as well as disturbing the function
11 of matrix metalloproteinase enzymes.³⁰ Another study shows the accumulation and oxidative
12 stress inflicted by SiQDs in gibel carp liver.³¹ Herein, bacteria was chosen as the model
13 microorganism for the nanotoxicity experiments, as they are at the base of the food web,
14 ubiquitous in the ecosystem, and have important roles in decomposition, nutrient cycling, and
15 bioremediation. *Shewanella oneidensis* MR-1, a Gram-negative bacterium, and *Bacillus subtilis*
16 SB491, a Gram-positive bacterium, are the two environmentally-beneficial representative
17 bacteria species employed in this work. *S. oneidensis* has shown minimal impact upon exposure
18 to engineered nanoparticles in previous studies, thus making it a robust bacteria model to screen
19 QDs for any possible toxic effects under chronic or high exposure dose conditions.³² Even
20 though the facultative anaerobic *S. oneidensis* is a known dissimilatory metal-reducing bacteria,
21 this ability is not relevant here because *S. oneidensis* is unlikely to respire by assimilating metals
22 in the Cd-based QDs in aerobic conditions,³³⁻³⁵ as used in the following studies. Additionally,
23 there are no reports of *S. oneidensis* being able to reduce silicon in either aerobic or anaerobic
24 conditions. *B. subtilis* is not a metal-reducing bacteria, and thus our studies provide an interesting
25 aspect of comparison with *S. oneidensis*. One Gram-negative and one Gram-positive bacterium
26
27
28
29
30
31
32
33
34
35
36
37
38
39
40
41
42
43
44
45
46
47
48
49
50
51
52
53
54
55
56
57
58
59
60

1
2
3 were chosen because they present distinct surface chemistry during QD exposure. Gram-negative
4 bacteria exhibit a double-membrane system, with two lipid membranes (outer and inner
5 cytoplasmic), which are separated by a thin peptidoglycan layer. Lipopolysaccharide molecules
6 are present on the outside of the outer membrane. The cell wall of a Gram-positive bacterium
7 comprises a single cytoplasmic lipid membrane with a thick exterior layer of peptidoglycan.
8 Teichoic and lipoteichoic acids are embedded within the peptidoglycan layer. By assessing QD
9 interaction with both Gram-negative and Gram-positive bacteria, this work moves towards
10 generalization of QD impacts based on bacterial membrane characteristics.
11
12
13
14
15
16
17
18
19
20
21
22
23

24 Briefly, this work demonstrates the effects of two Cd-containing QDs and SiQDs on the viability
25 of the Gram-negative bacteria *Shewanella oneidensis* MR-1 and the Gram-positive bacteria
26 *Bacillus subtilis* SB 491 using techniques such as colony counting, respirometry, and a
27 membrane integrity assay. This work also investigates the association of the QDs with the
28 bacterial cells using biological transmission electron microscopy (TEM). The CdSe QDs exhibit
29 significant toxicity towards the bacteria cells, but CdSe/ZnS and SiQDs are largely benign,
30 presenting two promising proactive design strategies for current and future technological
31 applications. The literature on QD toxicity is largely focused on mammalian models; it is
32 instructive to keep this literature in mind as an ecological system is considered here. A previous
33 study where rhesus macaques were treated with CdSe/CdS/ZnS QDs did not show any
34 evidence of toxicity, but showed the presence of Cd in organs even after 90 days after the
35 initial treatment.³⁶ Similar studies on mice and monkeys using SiQDs displayed no toxic
36 effects, but there was Si accumulation in the liver and spleen of the animals 3 months post-
37 treatment.³⁷ It's worth pointing out that the CdSe/ZnS QDs may exhibit delayed toxic effects
38
39
40
41
42
43
44
45
46
47
48
49
50
51
52
53
54
55
56
57
58
59
60

1
2
3 due to oxidation and dissolution of the ZnS shell and release of Cd^{2+} , and the limited time
4 exposure we have carried out with bacteria and QDs, may not be enough to rule out their
5 eventual toxicity. The benignness of SiQDs, even at high dosage as used in our studies, to
6 some extent rules out the negative effect of accumulated higher concentration of SiQDs. In the
7 future SiQDs can prove an extremely important alternative to all the Cd-based QDs, not only due
8 to their benign nature but also because they use only earth-abundant elements, as opposed to Cd-
9 based QDs.
10
11
12
13
14
15
16
17
18
19
20

21 **Methods:**

22 *Materials:* The SiQDs were synthesized as described below, while the CdSe QDs and CdSe/ZnS
23 core-shell QDs were purchased from NN-Labs. The CdSe/ZnS QD surfaces are functionalized
24 with a carboxylic acid ligand (listed in the catalog as item CZW), and the CdSe QDs were
25 custom-made by NN Labs, stabilizing them with the same carboxylic acid ligand.
26
27
28
29
30
31
32
33
34

35 *Synthesis of SiQDs:* SiQDs were synthesized in a low pressure, non-thermal plasma driven by a
36 13.56 MHz RF power source, nominally set to 60W. Silane (SiH_4) presented at 5% by volume in
37 helium was used as the silicon precursor at 14 sccm, while 10 sccm of argon acted as the
38 ionizing carrier gas. Both gases flew the entire length of a 9.5 mm outer diameter borosilicate
39 glass tube which expands to 25.6 mm outer diameter roughly 4 mm downstream of the powered
40 electrode.³⁸ Hydrogen was injected in this expanded afterglow region at a flow rate of 100
41 standard cubic centimeter per minute (sccm) to initially passivate the surface. The plasma
42 pressure was maintained at ~ 1.6 Torr via an orifice, after which particles were collected via
43 inertial impaction. These as-produced particles were then wetted with 0.2 mL of ethanol per 10
44
45
46
47
48
49
50
51
52
53
54
55
56
57
58
59
60

1
2
3 mg of silicon nanocrystals via sonication and subsequently diluted in an additional 1.8 mL of
4
5 deionized water and shaken. The solutions were then treated by an atmospheric pressure, non-
6
7 thermal microplasma jet to improve the dispersion of the hydrophobic particles in water.²⁸ The
8
9 radiofrequency driven microplasma used argon at a flow rate of 750 sccm was operated at an
10
11 average power of 2.5W. The nozzle of the jet was placed 3.5 mm above the water surface so that
12
13 the plasma plume touched the liquid surface. The volume of water was adjusted every 15
14
15 minutes to counter evaporation, and the total treatment time was 1 hour. After treatment, the
16
17 particles gain an oxide shell that improves the hydrophilicity.²⁸
18
19
20
21

22 *Characterization of QDs:*

23
24

25 The QDs were characterized using a combination of transmission electron microscopy (TEM),
26
27 UV-vis extinction spectroscopy, dynamic light scattering (DLS), and fluorescence spectroscopy.
28
29 TEM samples were prepared by dropcasting a small amount of the QD solution on a TEM grid,
30
31 drying the samples in ambient conditions, and images were acquired using an FEI Tecnai T12
32
33 TEM. SiQD samples were prepared for cryogenic TEM by administering 5 μ L onto a lacey
34
35 carbon grid, which was immediately dried and plunge frozen with a FEI Mark IV Vitrobot.
36
37 Samples were either deposited on hydrophobic grids or lacey carbon grids that were made
38
39 hydrophilic via glow discharge. Cryogenic TEM images were acquired on a Tecnai G2 Spirit
40
41 Biotwin. The hydrodynamic diameter of the SiQDs was determined via DLS on a Brookhaven
42
43 ZetaPALS instrument. This experiment was performed to assess the stability of the QDs in
44
45 bacterial media used for toxicity experiments. The fluorescence properties, including
46
47 excitation/emission spectra as well as quantum yield (QY) of the QDs, were assessed using a
48
49 calibrated integrating sphere paired with an Ocean Optics USB2000 spectrometer.
50
51
52
53
54
55
56
57
58
59
60

1
2
3 *Bacterial culture: Shewanella oneidensis* MR-1 stock was a gift from the lab of Jeff Gralnick at
4 the University of Minnesota. *Bacillus subtilis* strain SB 491 was purchased from Bacillus
5 Genetic Stock Center (Columbus, OH). The bacteria were stored at -80 °C before being
6 inoculated onto LB broth agar plates, which were incubated at 30 °C for *S. oneidensis* and 37 °C
7 for *B. subtilis*.

8
9
10
11
12
13
14
15
16
17 *Colony counting assays (Drop-plate and Pour-plate assays):* Colony counting experiments were
18 performed to assess the dose-dependent effect of the various QDs on both bacteria at 50 mg/L,
19 100 mg/L, and 200 mg/L QD concentrations. Bacteria liquid cultures were grown in Luria Broth
20 media (Difco LB Broth, Miller) for 4 h at 30 °C to mid-log phase from colony inoculants on
21 solid agar plates. Bacterial cells were harvested by centrifugation for 10 min at 2000xg, washed
22 in Dulbecco's phosphate-buffered saline (D-PBS) buffer, and suspended in a HEPES buffer (2
23 mM HEPES and 25 mM NaCl, at pH 7.4). The cultures were then diluted to OD 0.2 at 600 nm
24 (OD₆₀₀) to achieve a cell density of approximately 2×10^8 colony-forming units (CFUs)/mL.
25 Serial 10-fold dilutions of this bacterial suspension were performed at this stage to achieve a cell
26 concentration of 10^4 CFUs/mL in HEPES buffer. The resultant diluted bacteria suspension was
27 then treated with QDs at various concentrations (50 mg/L, 100 mg/L and 200 mg/L) and
28 incubated for 15 min. An adapted drop-plate method was used for the *S. oneidensis* cells, where
29 six 10 µL droplets of the exposed bacterial suspensions as well as untreated negative controls
30 were dropped on an LB-agar plate, which had been pre-sterilized under UV-illumination for 20
31 min. The droplets were dried under air flow in a biological cabinet and were incubated at 30 °C
32 for 20 hours before colonies were counted using a Bantex Colony Counter 920A. The viability of
33 cells from each treatment was reported as a ratio to the control samples. Due to the high motility
34
35
36
37
38
39
40
41
42
43
44
45
46
47
48
49
50
51
52
53
54
55
56
57
58
59
60

1
2
3 and swarming mobility of *B. subtilis* cells, the pour plate method of colony counting was
4 employed instead of the typical drop plate method. In this method, 60 μL of QD-incubated
5 bacterial cell suspension was placed in each well of a 12-well plate, and 1 mL of melted LB-agar
6 solution at 45 $^{\circ}\text{C}$ (1.5% agar) was poured and mixed well. The well plates were incubated at 37
7 $^{\circ}\text{C}$ for 20 hours, and the colonies in each well were counted. The viability of cells from each
8 treatment was reported as a ratio of number of colonies counted to the control samples. The
9 experiments were done using three different batches of SiQDs, and two different batches of Cd-
10 based QDs, and repeated three times (three biological replicates) for each batch of QDs.
11
12
13
14
15
16
17
18
19
20
21
22
23

24 *Respirometry*: Aqueous minimal media (buffered with 10 mM HEPES and containing 11.6 mM
25 NaCl, 4.0 mM KCl, 1.4 mM $\text{MgCl}_2 \cdot 6\text{H}_2\text{O}$, 2.8 mM Na_2SO_4 , 2.8 mM NH_4Cl , 0.088 mM
26 Na_2HPO_4 , 0.051 mM CaCl_2 , and 100 mM sodium lactate for *S. oneidensis* or 10 mM dextrose for
27 *B. subtilis*) was used to culture bacteria for 24 h. The concentration of the cell suspension was
28 modified to OD 0.2 at 600 nm (OD600) to achieve a cell density of approximately 2×10^8
29 CFUs/mL, and then further diluted 10-fold in minimal media. Aliquots of this diluted cell
30 suspension were pipetted into 125 mL respirometry glass bottles containing removable rubber
31 septa, and QD samples were introduced to achieve the desired QD exposure concentrations of 50
32 mg/L, 100 mg/L and 200 mg/L in a final exposure volume of 100 mL. As aerobic respiration
33 entails consumption of $\text{O}_2(\text{g})$ and generation of $\text{CO}_2(\text{g})$, KOH(aq.) inserts were placed into the
34 headspace above the culture, to remove the resulting CO_2 . The glass bottles were placed in a
35 water bath maintained at 30 $^{\circ}\text{C}$ for *S. oneidensis* and 37 $^{\circ}\text{C}$ for *B. subtilis*, and the suspensions
36 were stirred continuously at 500 rpm. A small gauge needle was placed through each septum,
37 and tubing (Tygon® 4040-A) linked each bottle to a respirometer system (Respirometer Systems
38
39
40
41
42
43
44
45
46
47
48
49
50
51
52
53
54
55
56
57
58
59
60

1
2
3 and Applications, Inc., Springdale, AK) that monitored cellular $O_{2(g)}$ consumption over 24 h. As
4
5 the cell population size increases over time, total aerobic respiratory activity also should
6
7 increase. Aerobic respiration decreases the total $O_{2(g)}$ pressure in the headspace of the sealed
8
9 bottles, and $O_{2(g)}$ was supplied as needed at 10 min intervals to maintain a constant pressure. The
10
11 total mass of $O_{2(g)}$ delivered to each vessel was recorded at 10 min intervals over 24 h.
12
13

14
15
16 *Membrane integrity assay (Live-Dead assay kit)*: In parallel to the colony counting and
17
18 respirometry measurements, the integrity of bacterial cell membranes was also monitored. A
19
20 fluorescent LIVE/DEAD™ BacLight Bacterial Viability Kit containing two nucleic acid stains,
21
22 propidium iodide (PI) and SYTO9, was used to evaluate the “live:dead ratio” which is the ratio
23
24 of cells with intact cell membranes to cells with compromised cell membranes. SYTO9 is a cell
25
26 permeant, intercalating nucleic acid stain that can stain all the bacterial cells in suspension,
27
28 whereas PI is a cell impermeant nucleic acid stain that only associates with cells that have
29
30 damaged cell membranes. For this experiment, bacteria (either *S. oneidensis* or *B. subtilis*) were
31
32 incubated in LB broth overnight, and diluted to OD 0.2 at 600 nm (OD600) to achieve a cell
33
34 density of approximately 2×10^8 CFUs/mL in HEPES after a washing step with DPBS. The
35
36 diluted bacteria were incubated with QDs at 50 mg/L, 100 mg/L, or 200 mg/L resultant
37
38 concentrations for time periods of 1 h or 6 h. 100 μ L of bacteria samples were aliquoted into a
39
40 96-well plate, then mixed with the 100 μ L of dye mixture containing both SYTO9 and PI, and
41
42 fluorescence measurements were collected in a Synergy 2 Multi-Mode Microplate Reader
43
44 (BioTek, VT). The sample mixture was excited at 485 nm, and emission data was collected at
45
46 528 nm for SYTO9 and 635 nm for PI. The emission data for both SYTO9 (indicating “live”
47
48 cells) and PI (indicating “dead” cells) were normalized to their respective negative controls, and
49
50 the ratio of these normalized data indicate the “live:dead ratio”.
51
52
53
54
55
56
57
58
59
60

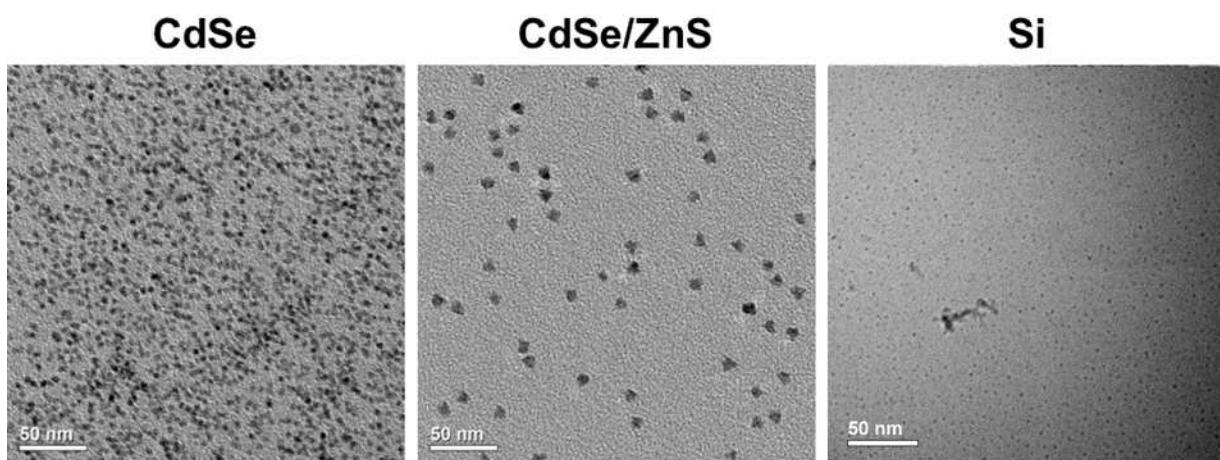
1
2
3
4
5 *Biological TEM analysis:* Bacteria were cultured in LB broth overnight, then diluted to an OD of
6 0.8 at 600 nm in HEPES. The diluted bacterial suspension was centrifuged down to a pellet,
7
8 washed thrice with 0.1 M cacodylate buffer solution, then resuspended in a fixation buffer of
9
10 2.5% glutaraldehyde in 0.1 M sodium cacodylate buffer and fixed for 50 minutes. The pellet was
11
12 washed with sodium cacodylate buffer, and dehydrated stepwise with increasing concentration of
13
14 ethanol (30, 50, 70, 80, 90, 95, and 100% ethanol in water). After removing the last ethanol
15
16 rinse, the pellet was washed with propylene oxide three times, and the infiltration steps were
17
18 carried out. The pellet was soaked for 2 h in a 2:1 propylene oxide:epoxy resin mixture. This was
19
20 replaced with a 1:1 propylene oxide: epoxy resin mixture, and the pellet was incubated in this
21
22 mixture overnight. After this, the pellet was incubated in a fresh batch of 1:1 propylene oxide:
23
24 epoxy resin mixture for 6 h, and finally placed in a pure resin mixture and infiltrated overnight.
25
26 The resin sample was then cured in a 40 °C oven for one day and then 60 °C oven for two days.
27
28 Ultrathin sections (65 nm) were sectioned by using Leica UC6 microtome and Diatome diamond
29
30 knife, then stained with uranyl acetate and lead citrate. These sections were placed on copper
31
32 TEM grids (Ted Pella Inc.), and imaging was done using an FEI Tecnai T12 TEM.
33
34
35
36
37
38
39
40

41 **Results and discussion:**

42 *Characterization of QDs:*

43
44
45 *Physical characterization:* Figure 1 shows the TEM images of the three QDs compared herein:
46
47 CdSe, CdSe/ZnS and SiQDs. The approximate diameter of the CdSe QDs, as provided by the
48
49 manufacturer, is 4.6 nm, and that of the CdSe/ZnS QDs is roughly 9 nm total with a 4.5 nm core.
50
51 It was difficult to assess the exact size of the SiQDs using TEM images due to the extensive
52
53 aggregation; hence, cryogenic TEM images were acquired to observe SiQDs in vitrified water.
54
55
56
57
58
59
60

1
2
3 When SiQDs were deposited on hydrophilic grids, particles had an average diameter of
4 3.8 ± 0.04 nm ($n=400$, mean \pm std. error). Larger aggregates were observed on both hydrophobic
5 3.8 ± 0.04 nm ($n=400$, mean \pm std. error). Larger aggregates were observed on both hydrophobic
6 and hydrophilic grids with average diameters of 19.2 ± 0.2 nm ($n=300$, mean \pm std. error). DLS
7 experiments were performed to evaluate the hydrodynamic diameters of the SiQD aggregates
8 both in water and HEPES buffer (the media used for biological exposures). The measurements
9 were done at SiQD concentrations of 50 mg/L, 100 mg/L, and 200 mg/L to monitor not only the
10 effect of the incubating media, but also QD concentration on aggregate size. These results are
11 shown in Figure 2. In the DLS data, the SiQDs exhibit very large aggregate formation in both
12 Milli-Q water and HEPES (4-(2-hydroxyethyl)-1-piperazineethanesulfonic acid) media.
13 However, no significant difference in aggregate size was observed when comparing the data in
14 Milli-Q water and HEPES or at the different concentrations. The zeta potential of the SiQDs was
15 measured to be -13.2 ± 0.3 mV. This low magnitude zeta potential likely contributes to the
16 colloidal instability of the SiQDs in dispersion.³⁹
17
18
19
20
21
22
23
24
25
26
27
28
29
30
31
32
33
34
35



50
51
52 *Figure 1: Representative transmission electron micrographs of CdSe, CdSe/ZnS and cryogenic*
53 *transmission electron micrographs of SiQDs*
54
55
56
57
58
59
60

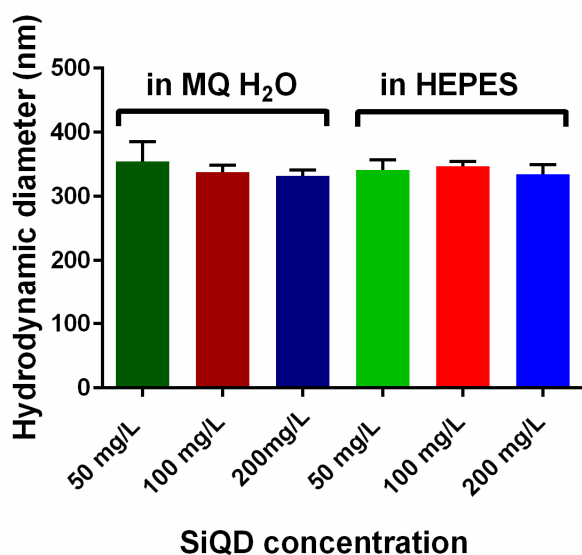
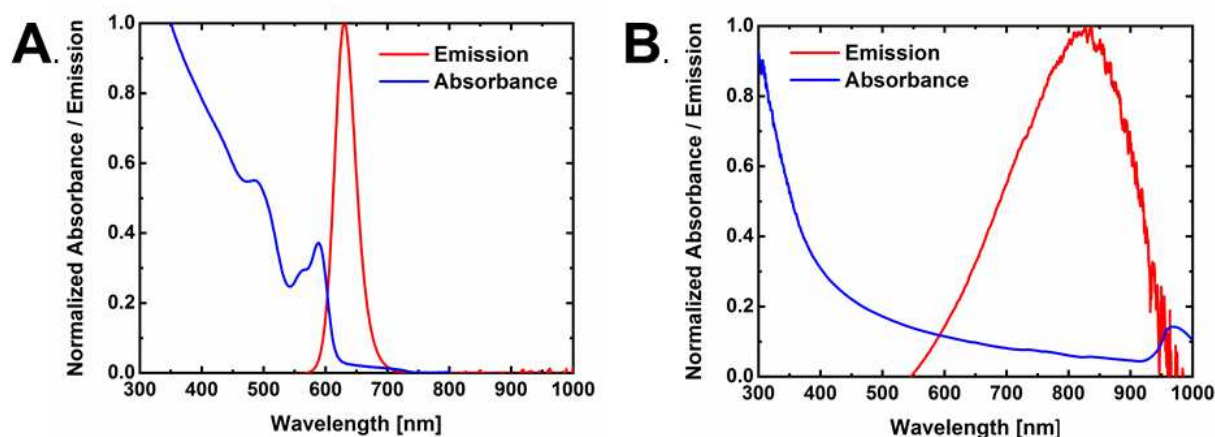


Figure 2: Hydrodynamic diameter of the SiQDs in MQ H₂O and HEPES buffer obtained by dynamic light scattering. No significant difference in hydrodynamic diameter is observed for the two media or among different nanoparticle concentrations used. The error bars indicate standard deviation using three measurements.

Optical characterization: To investigate the optical properties of the QDs, UV-vis extinction, steady-state emission, and absolute quantum yield (AQY) measurements were completed. The emission spectra and AQY were measured using a calibrated integrating sphere paired with an Ocean Optics USB2000 spectrometer. The measurement methods are described by Mangolini et al.⁴⁰ with excitation provided by a 395 nm LED. The CdSe cores exhibited observable absorption signals at 500 nm and 590 nm, similar to the CdSe/ZnS QDs absorption in Figure 3A. However, as the surface defects were not passivated by a protective shell, namely the ZnS layer, the photoluminescence of CdSe QDs were quenched significantly.⁴¹ Therefore, the CdSe QDs did not exhibit bright enough emission to be detected by our spectrometer. The CdS/ZnS QDs exhibited an emission peak at 630 nm (Figure 3A) and their AQY was 47%, whereas SiQDs exhibited an emission peak near 830 nm (Figure 3B), and their AQY was measured to be 25%. Because of the near infrared (NIR) limitations of our spectrometer, it is possible the broad SiQD emission actually extends further to NIR. If so, the AQY would be greater than measured and the

1
2
3 reported value can be considered a lower bound. The peak emission of the CdSe/ZnS at 630 nm
4 corresponds to a red-orange color, while the peak of the SiQDs at 830 nm is in the near infrared,
5 rather than the visible. The SiQDs synthesized in a plasma reactor can provide an inexpensive
6 and potentially environment-friendly alternative to Cd-based QDs, though further optimization
7 needs to be done to reach quantum yields that match their Cd-containing counterparts.
8
9
10
11
12
13
14



15
16
17
18
19
20
21
22
23
24
25
26
27
28
29
30
31
32
33
34
35
36
37
38
39
40
41
42
43
44
45
46
47
48
49
50
51
52
53
54
55
56
57
58
59
60

Figure 3: A) Optical properties (UV-vis absorption and emission) of CdSe/ZnS QDs and (B) optical properties (UV-vis absorption, and emission) of SiQDs.

Comparative toxicity assessment of QDs:

Colony counting assays (Drop-plate and Pour-plate assays):

Colony counting assays have been considered a gold standard in bacterial cell enumeration in microbiology. In this work, colony counting assays were used to determine the number of viable bacteria cells in a solution after they had been treated with the different QDs (CdSe, CdSe/ZnS, or Si). The bacteria solution was diluted to obtain discrete and non-overlapping colonies on the LB-agar plate. The diluted bacterial suspension was exposed to increasing QD concentration to assess the dose-dependent nature of any toxicity that the QDs exhibit. These solutions were plated on LB-agar plates and incubated for 18-20 h so that countable colonies were discernible. The number of colonies formed on the LB-agar plate indicate the number of viable cells present

1
2
3 in the exposure solution. Thus, any decrease in the number of colonies compared to the negative
4 control was attributed to toxic effects exhibited by the QDs. The drop plate colony counting
5 method was used for the Gram-negative bacteria *Shewanella oneidensis* MR-1, and the pour
6 plate colony counting method was employed for the Gram-positive bacteria *Bacillus subtilis*
7 SB491.
8
9
10
11
12
13

14
15
16
17 The results of the drop plate colony counting assays with *Shewanella oneidensis* following
18 exposure to QD concentrations of 50 mg/L, 100 mg/L, or 200 mg/L are shown in Figure 4. The
19 results for parallel pour plate colony counting assays with *Bacillus subtilis* are shown in Figure 5.
20
21 Statistical analysis was performed using one-way ANOVA, followed by post-hoc Tukey's
22 multiple comparisons tests (GraphPad Prism software, La Jolla, CA). All values plotted are the
23 mean \pm standard deviation (SD), and statistical significance is indicated using asterisks (p values
24 < 0.0001 indicated by ****, 0.0001 to 0.001 indicated by ***, 0.001 to 0.01 indicated by **, and
25 0.01 to 0.05 indicated by *).
26
27
28
29
30
31
32
33
34
35
36
37

38 The SiQDs did not have any significant toxic impact on either *S. oneidensis* or *B. subtilis* cells at
39 any of the tested concentrations. The CdSe QDs were significantly more toxic to the bacteria
40 cells, when compared to the SiQDs or the CdSe/ZnS QDs. At a concentration of 200 mg/L, the
41 CdSe QDs killed about 95% of the cells in case of *S. oneidensis* and 75% cells in case of *B.*
42 *subtilis*. The CdSe/ZnS QDs were not toxic to *S. oneidensis* cells at any of the concentrations
43 considered, but showed mild toxicity to the *B. subtilis* cells at 200 mg/L. Cd-based QDs can
44 exhibit toxicity due the effect of dissolved toxic Cd(II) ions,^{42,43} as well as the generation of
45 reactive oxygen species (ROS).^{44,45, 24} ROS is known to induce growth defects in bacteria,
46
47
48
49
50
51
52
53
54
55
56
57
58
59
60

1
2
3 inactivate mononuclear iron proteins, cause DNA damage, oxidize cysteine proteins, and
4 peroxidize lipids, amongst other effects.⁴⁶ Reactive oxygen species (ROS) produced in cells by
5 heavy metal stresses are known to damage iron-containing proteins in *S. oneidensis*.⁴⁷ Cd(II)
6 ions can impact biological systems in several ways: (1) by inhibiting DNA repair mechanisms by
7 impairing the damage recognition step⁴⁸ (2) by causing oxidative stress in cells through ROS
8 generation, and subsequent damage to cell membranes,⁴⁹ and (3) by incorporating into Gram-
9 negative cells through the Mg(II) uptake system or Gram-positive cells by the Mn(II) uptake
10 system.⁵⁰ The ZnS shell on the CdSe core can mitigate some of the toxicity of the cores⁴² by
11 protecting the cores from weathering and oxidation and eventual dissolution to Cd(II) ions.²
12 Despite the protective shell, some toxic effect was observed for the *B. subtilis* cells when treated
13 with 200 mg/L CdSe/ZnS QDs. Gram-positive bacteria, like *B. subtilis*, can be more susceptible
14 to toxicity posed by nanoparticles than Gram-negative bacteria, like *S. oneidensis*, because they
15 lack an outer cell membrane with lipopolysaccharide (LPS) chains that play a protective role.⁵¹
16
17
18
19
20
21
22
23
24
25
26
27
28
29
30
31
32
33
34
35
36
37
38
39
40
41
42
43
44
45
46
47
48
49
50
51
52
53
54
55
56
57
58
59
60

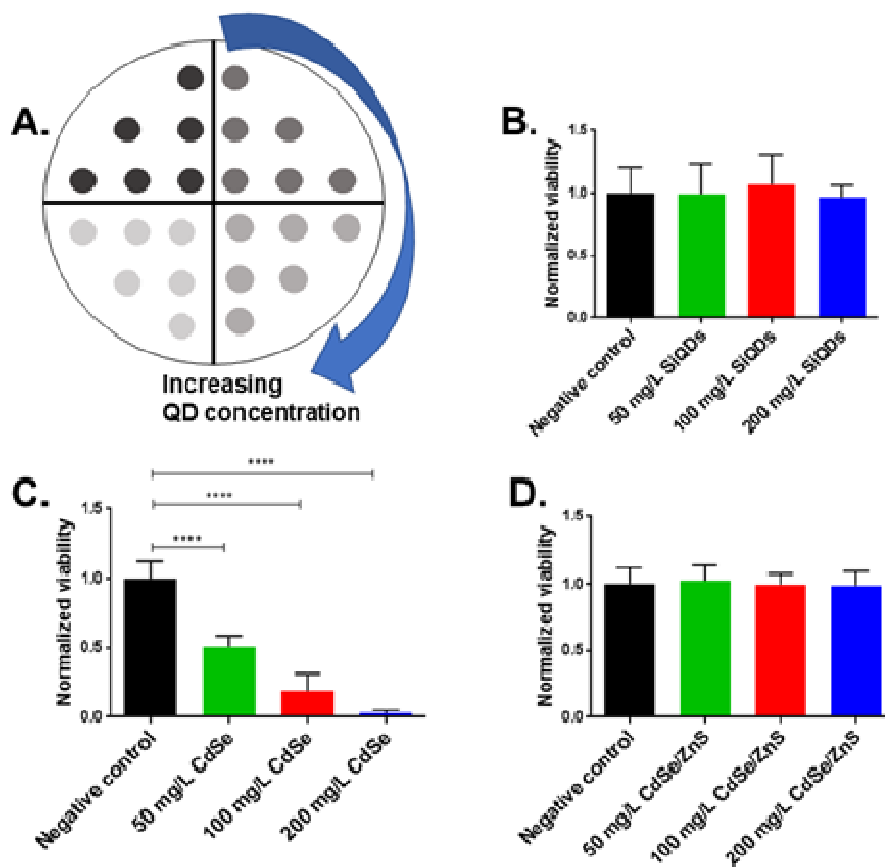


Figure 4: Bacterial viability of *S. oneidensis* assessed using drop plate colony counting. A. The template of an LB-agar plate for drop plate assay B. No observable effect on bacterial viability with treatment with SiQDs C. Significant dose-dependent toxic effect when treated with CdSe QDs D. No effect on bacterial viability upon exposure to CdSe/ZnS QDs. The error bars denote the standard deviation between three biological replicates. p values < 0.0001 indicated by ****.

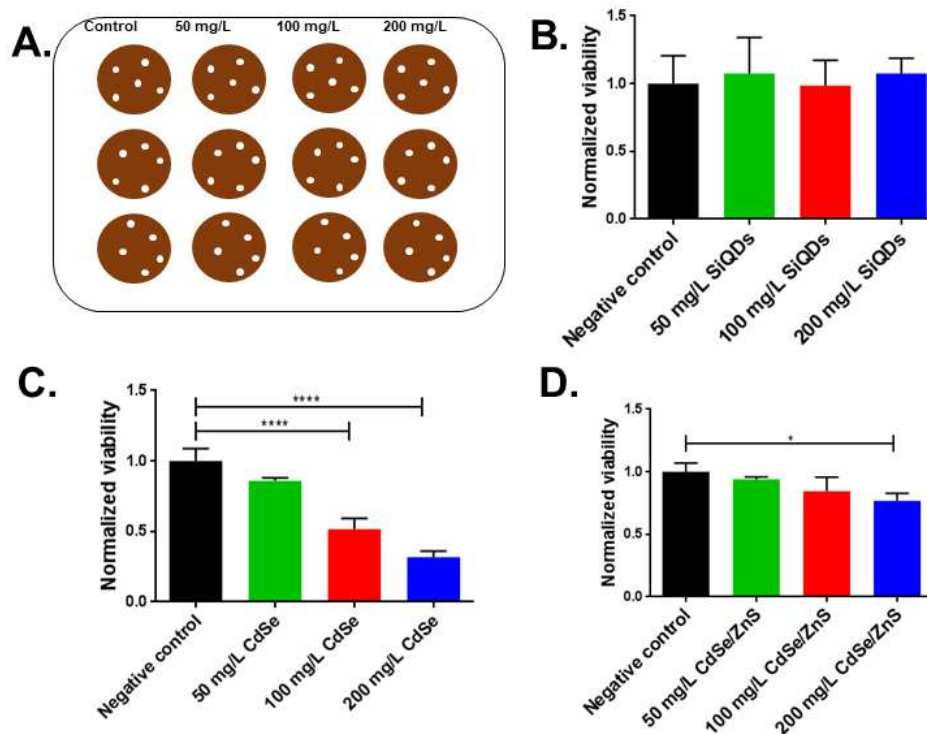
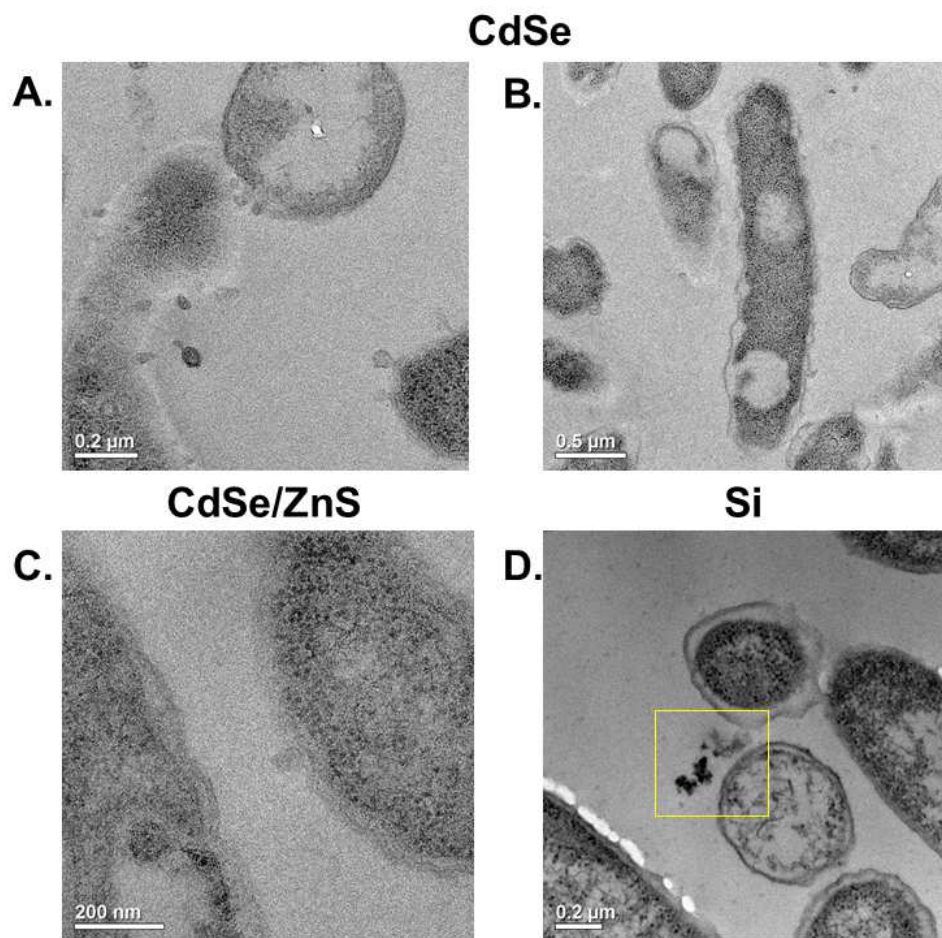


Figure 5: Bacterial viability of *B. subtilis* assessed using pour plate colony counting. A. The template of a 12-well plate for pour plate assay B. No observable bactericidal effect on treatment with SiQDs C. Significant dose-dependent toxic effect when treated with CdSe QDs D. Small effects on bacterial viability upon exposure to CdSe/ZnS QDs. The error bars denote the standard deviation between three biological replicates. p values < 0.0001 indicated by ****, and 0.01 to 0.05 indicated by *Biological TEM analysis:

Biological TEM imaging provides qualitative insight into the spatial interactions between bacterial cells and QDs after the cells have been incubated with the QDs. Figure 6 shows the results obtained from imaging *S. oneidensis* samples exposed to the three different QDs at 200 mg/L for 15 minutes. The CdSe-treated *S. oneidensis* cells show significantly damaged cell membrane structures, and many polyp-like globules of disintegrated cell membranes far from their original location (Figure 6A). One interesting feature present in the CdSe-exposed *S. oneidensis* samples was the abnormal elongation of the bacterial cells (Figure 6B). Similar results have been observed previously with *S. oneidensis* cells incubated with CdTe QDs.⁵² This abnormal elongation is a known phenomenon in bacteria cells called filamentation. This occurs when a cell continues to elongate but does not undergo cell division due to inhibition of chromosome replication caused by DNA damage.⁵³ The presence of filamentous cells in the

1
2
3 sample suggests DNA damage and genotoxicity to *S. oneidensis* cells in the presence of CdSe
4 QDs. This can be directly correlated with the cell viability data obtained from the colony-
5 counting assay. Neither the CdSe nor the CdSe/ZnS QDs were observed near any of the *S.*
6
7
8
9
10 *oneidensis* cells.



43 *Figure 6: Biological transmission electron micrographs for S. oneidensis after treatment with*
44 *QDs. A. & B. TEM images of B. subtilis treated with CdSe QDs. Indicate the cell membrane*
45 *damage and filamentation of bacterial cells following exposure to CdSe QDs. C. TEM images of*
46 *B. subtilis treated with CdSe/ZnS QDs. Indicates no association of CdSe/ZnS QDs with bacterial*
47 *cells. D. TEM images of B. subtilis treated with SiQDs. Indicates no association of SiQDs with*
48 *bacterial cells although the presence of SiQD aggregates is apparent (indicated by yellow box).*
49

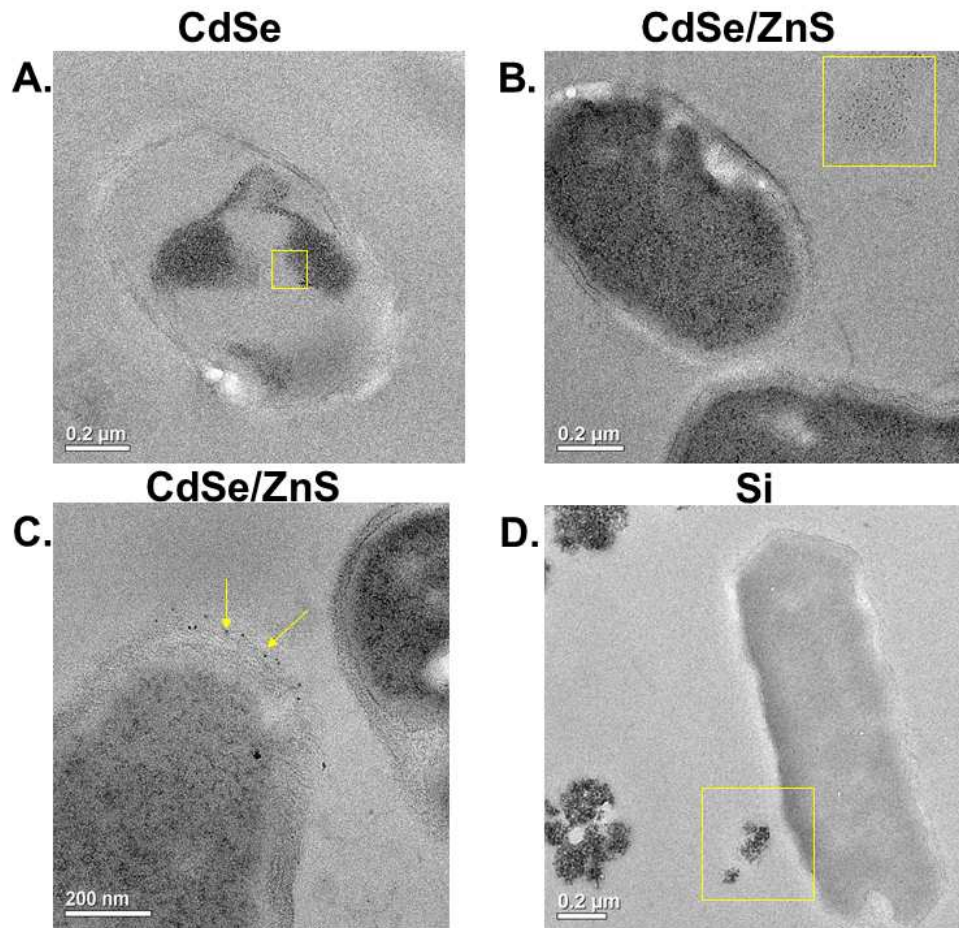


Figure 7: Biological TEM for *B. subtilis* after treatment with QDs. A TEM images of *B. subtilis* treated with CdSe QDs. Indicate the cell membrane damage of bacterial cells following exposure to CdSe QDs. The yellow box indicates CdSe QDs associated with cellular material. B. & C. TEM images of *B. subtilis* treated with CdSe/ZnS QDs. No association of CdSe/ZnS QDs with the majority of bacterial cells. Cell membrane damage and association observed in some cells as denoted by yellow arrows in 7C. D. TEM images of *B. subtilis* treated with SiQDs. No association of SiQDs with bacterial cells as denoted by SiQD aggregates in the box in 7D.

Neither the CdSe/ZnS nor the SiQDs exhibited any noticeable qualitative association with or impact on the *S. oneidensis* cells. For the sample containing the SiQDs, the QDs were aggregated near the cells, but no direct contact between the QDs and the cells were observed after visualizing a minimum of 20 bacterial cells across 2 TEM grids. For the *B. subtilis* cells, cell membrane damage was observed following treatment with CdSe QDs. A majority of the cells

1
2
3 treated with CdSe/ZnS QDs appear intact, with no association with the QDs (Figure 7B);
4
5 however, a few cells showed localized cell membrane damage, with QDs dotted along the
6
7 compromised cell wall (Figure 7C). No interaction between the SiQDs and *B. subtilis* cells was
8
9 noted. (Figure 7D)
10
11
12
13

14 *Further toxicity assessment of SiQDs:* Due to the novel nature of the SiQDs used in this study,
15
16 and the lack of previous studies on toxicity assessment of Si-based QDs, further experiments
17
18 were performed to probe any possible sub-lethal effects of the SiQDs on the two model bacteria,
19
20 *S. oneidensis* and *B. subtilis*. The effect of the SiQDs on bacterial respiration and oxygen uptake
21
22 was assessed using respirometry, and the membrane integrity in presence of the SiQDs was
23
24 monitored using the Live-Dead *BacLight* assay kit.
25
26
27
28
29

30
31 *Respirometry:* The oxygen consumption of bacterial cells over time was examined using a
32
33 respirometer. Any sub-lethal impact due to the QDs, such as delayed onset of growth, can be
34
35 assessed from the oxygen uptake curve. The oxygen uptake curve generally follows a sigmoidal
36
37 shape, like the bacterial growth curve, since the population growth and oxygen uptake are
38
39 proportional to one another. With one biological replicate for each of the two materials
40
41 replicates, neither the 50 nor 100 mg/L SiQDs had significant effects on the respiration of either
42
43 *S. oneidensis* or *B. subtilis* cells (Figure 8).
44
45
46
47
48
49
50
51
52
53
54
55
56
57
58
59
60

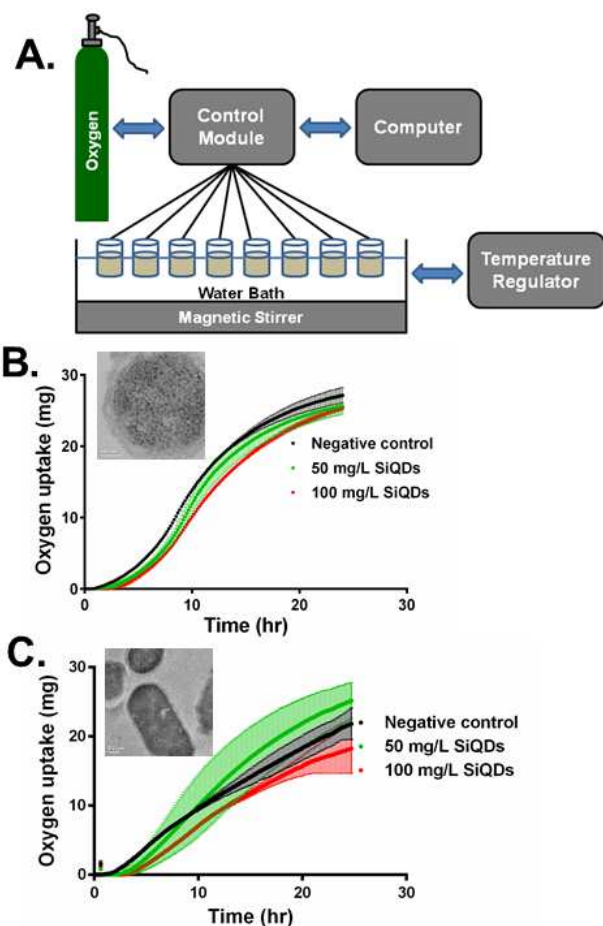


Figure 8: A. Schematic of the respirometer setup. B. Representative respirometry data for *S. oneidensis* and C. *B. subtilis*. Both the negative control and SiQD-exposures to 50 and 100 mg/L are shown.

Membrane integrity assay (Live-Dead assay kit): The membrane integrity assay using the Live-Dead BacLight assay kit employs two nucleic acid stains: green fluorescing SYTO-9, which stains all cells, and red fluorescing propidium iodide, which penetrates and stains cells with compromised membranes. A decreased green/red fluorescence ratio indicates a more permeable membrane. The experiment was done by treating the bacteria cells with QDs for 1 h or 6 h time periods, introducing the dye mixture, and then measuring the fluorescence data. The results show minimal effect of the SiQDs on the cell membrane integrity for both bacteria species. Even at an extended exposure time of 6 h, there was no significant change in the “live:dead ratio” compared

to the negative control. Thus, it can be concluded that the SiQDs do not damage the cell membrane of the bacteria.

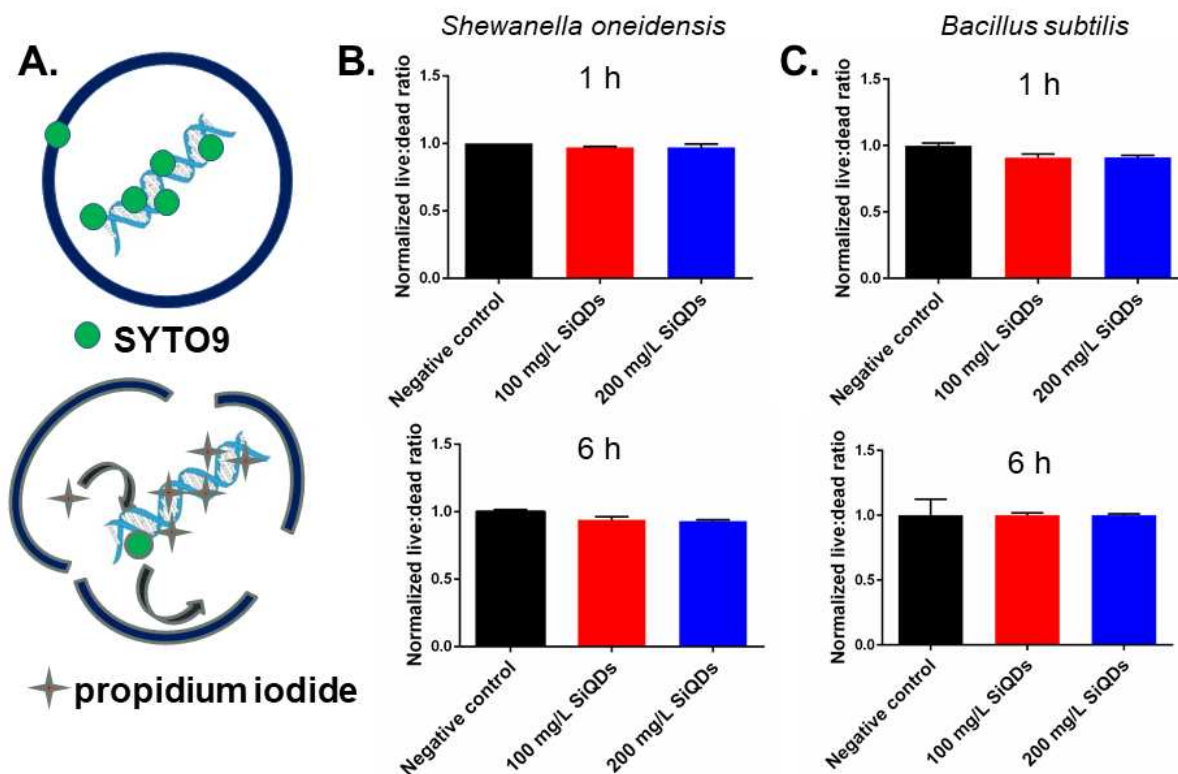


Figure 9: Live-dead membrane integrity assay with bacteria and QDs. A. Schematic showing cell permeable SYTO9 and cell impermeable propidium iodide (PI). B. Data for *S. oneidensis* after 1 h and 6 h treatment with Si QDs C. Data for *B. subtilis* after 1 h and 6 h treatment with Si QDs. The error bars denote the standard deviation between two biological replicates.

Conclusions:

SiQDs with good optical properties were synthesized in a low-pressure, non-thermal plasma, and then treated with a microplasma to make them water dispersible. These QDs, made of earth-abundant silicon, have potential as a sustainable alternative to transition metal-based QDs. This

1
2
3 work set out to consider potential toxicity of these materials to bacteria, critical components of
4 the food web. The effects of the SiQDs were considered on two different bacteria, one Gram-
5 negative and the other Gram-positive, and compared with the effects of two traditional Cd-based
6 QDs (CdSe and CdSe/ZnS). The SiQDs did not show any effect on the viability of bacteria cells
7 as seen in the colony counting assays, whereas the CdSe QDs exhibited significant dose-
8 dependent toxic effects on the bacteria. The ZnS-coated CdSe QDs showed little to no toxicity to
9 the two bacteria tested. In biological TEM studies the SiQDs showed no association or
10 qualitative impact on bacterial morphology while the CdSe-treated bacteria showed cell
11 membrane damage and filamentation. The ZnS-coated CdSe QDs were seen to exhibit minimal
12 association with the *B. subtilis* cells. Upon exploration of more nuanced bacterial impacts, the
13 SiQDs proved to be benign when considering both respiration and membrane integrity. Overall,
14 based on considerations of bacterial toxicity, this work supports SiQDs as a non-toxic, benign
15 alternative to Cd-based QDs, with the potential to reach comparable luminescent properties.
16 While adding a shell to traditional CdSe QDs appears to be similarly benign, the SiQDs have the
17 additional benefit of being synthesized from an earth-abundant material with more mature
18 recycling infrastructure.^{54,55}

41 42 **Acknowledgements:**

43
44
45 This work was supported primarily by the National Science Foundation through the University
46 of Minnesota MRSEC under Award Number DMR-1420013. Part of this work was carried out in
47 the College of Science and Engineering Characterization Facility, University of Minnesota,
48 which has received capital equipment funding from the NSF through the UMN MRSEC program
49 under Award Number DMR-1420013. SKEH acknowledges support through the NSF Graduate
50
51
52
53
54
55
56
57
58
59
60

1
2
3 Research Fellowship Program under grant NSF GRFP 00039202. NVH acknowledges support
4 through the National Science Foundation Graduate Research Fellowship Program. JNW
5 acknowledges UMN MRSEC REU Site in Nanomaterials supported through the National
6 Science Foundation MRSEC and REU programs under Award Numbers DMR-1263062 &
7 DMR-1420013. EAM acknowledges Lloyd W. Goerke scholarship and the M. Cannon Sneed
8 Memorial award through the UMN Department of Chemistry. The authors would like to thank
9 Fang Zhou for microtoming the biological TEM samples and Guillermo Marqués and the
10 University Imaging Centers at the University of Minnesota for their help with acquiring
11 fluorescence microscopy images.
12
13
14
15
16
17
18
19
20
21
22
23
24
25

26 References:

- 27 (1) P. V. Kamat, Quantum dots continue to shine brightly, *J. Phys. Chem. Lett.*, 2016, **7**,
28 584–585.
29
- 30 (2) B. O. Dabbousi, F. V. Mikulec, J. R. Heine, H. Mattoussi, R. Ober, K. F. Jensen and M.
31 G. Bawendi, (CdSe) ZnS core - shell quantum dots : Synthesis and characterization of a
32 size series of highly luminescent nanocrystallites, *J. Phys. Chem.B*, 1997, **101**, 9463–
33 9475.
34
- 35 (3) E. R. Goldman and H. Mattoussi, Quantum dot bioconjugates for imaging , labelling and
36 sensing, *Nat. Mater.*, 2005, **4**, 435–446.
37
- 38 (4) B. Zorman, T. M. V. Ramakrishna and R. A. Friesner, Quantum confinement effects in
39 CdSe quantum dots, *J. Phys. Chem.*, 1995, **99**, 7649–7653.
40
- 41 (5) T. Kim, C. Cho, B. Kim and S. Park, Quantum confinement effect in crystalline silicon
42 quantum dots in silicon nitride grown using and quantum confinement effect in crystalline
43
44
45
46
47
48
49
50
51
52
53
54
55
56
57
58
59
60

- 1
2
3 silicon quantum dots in silicon nitride grown using SiH₄ and NH₃, *Appl. Phys. Lett.*, 2006,
4
5 **88**, 123102-1-3.
6
7
8 (6) A. I. Ekimov and A. A. Onushchenko, Quantum size effect in three dimensional
9
10 microscopic semiconductor crystals, *JETP Lett.*, 1981, **34**, 345–349.
11
12 (7) Y. Shirasaki, G. J. Supran, M. G. Bawendi and V. Bulović, Emergence of colloidal
13
14 quantum-dot light-emitting technologies, *Nat. Photonics*, 2013, **7**, 13-23.
15
16 (8) P. Reiss, M. Protière and L. Li, Core / shell semiconductor nanocrystals, *Small*, 2009, **5**,
17
18 154-168.
19
20
21
22 (9) D. Vasudevan, R. R. Gaddam, A. Trinchi and I. Cole, Core-shell quantum dots
23
24 Properties and applications, *J. Alloys Compd.*, 2015, **636**, 395–404.
25
26
27
28 (10) W. C. W. Chan, D. J. Maxwell, X. Gao, R. E. Bailey, M. Han and S. Nie, Luminescent
29
30 quantum dots for multiplexed biological detection and imaging, *Curr Opin*
31
32 *Biotechnol.*, 2002, **13**, 40-46.
33
34
35 (11) G. Xu, S. Zeng, B. Zhang, M. T. Swihart, K. Yong and P. N. Prasad, New generation
36
37 cadmium-free quantum dots for biophotonics and nanomedicine, *Chem Rev.*, 2016, **116**,
38
39 12234-12327.
40
41
42 (12) P. Bhattacharya, S. Ghosh and A. D. Stiff-Roberts, Quantum dot opto-electronic devices,
43
44 *Annu. Rev. Mater. Res.*, 2004, **34**, 1–40.
45
46
47 (13) Y. Yang, Y. Zheng, W. Cao, A. Titov, J. Hyvonen, J. R. Manders, J. Xue, P. H. Holloway
48
49 and L. Qian, High-efficiency light-emitting devices based on quantum dots with tailored
50
51 nanostructures, *Nat. Photonics*, 2015, **9**, 259–266.
52
53
54 (14) S. J. Rosenthal, J. C. Chang, O. Kovtun, J. R. McBride and I. D.
55
56 Tomlinson, Biocompatible quantum dots for biological applications, *Chem. Biol.*, 2011,
57
58
59
60

- 1
2
3 **18**, 10–24.
4
5
6 (15) A. P. Alivisatos, W. Gu and C. Larabell, Quantum dots as cellular probes, *Annu. Rev.*
7
8 *Biomed. Eng.*, 2005, **7**, 55–76.
9
10 (16) D. Bimberg, Quantum dots for lasers , amplifiers and computing, *J. Phys. D: Appl. Phys.*,
11
12 2005, **38**, 2055–2058.
13
14 (17) K. Bourzac, Quantum dots go on display. *Nature* **493**, 283(17 January 2013).
15
16
17
18 (18) C. P. Baldé, F. Wang, R. Kuehr, J. Huisman, 2015, The global e-waste monitor – 2014,
19
20 United Nations University, IAS – SCYCLE, Bonn, Germany.
21
22 (19) R. Hardman, A toxicologic review of quantum dots : Toxicity depends on
23
24 physicochemical and environmental Factors, *Environ. Health Perspect.*, 2006, **114**, 165–
25
26 172.
27
28
29 (20) J. L. Pelley, A. S. Daar and M. A. Saner, State of academic knowledge on toxicity and
30
31 biological fate of quantum dots, *Toxicol. Sci.*, 2009, **112**, 276–296.
32
33 (21) N. Chen, Y. He, Y. Su, X. Li, Q. Huang, H. Wang, X. Zhang, R. Tai and C. Fan, The
34
35 cytotoxicity of cadmium-Based quantum dots, *Biomaterials*, 2012, **33**, 1238–1244.
36
37 (22) B. I. Ipe, M. Lehnig and C. M. Niemeyer, On the generation of free radical species from
38
39 quantum dots, *Small*, 2005, **1**, 706–709.
40
41 (23) M. Green and E. Howman, Semiconductor quantum dots and free radical induced DNA
42
43 nicking, *Chem. Commun.*, 2005, **0**, 121-123.
44
45 (24) Z. Lu, C. M. Li, H. Bao, Y. Qiao and Y. Toh, Mechanism of antimicrobial activity of
46
47 CdTe quantum dots, *Langmuir*, 2008, **24**, 5445–5452.
48
49 (25) E. Morelli, E. Salvadori, R. Bizzarri, P. Cioni and E. Gabellieri, Interaction of CdSe / ZnS
50
51 quantum dots with the marine diatom *Phaeodactylum tricorutum* and the green alga
52
53
54
55
56
57
58
59
60

- 1
2
3 *Dunaliella tertiolecta* : A biophysical approach, *Biophysical Chemistry*, 2013, **182**, 4–10.
- 4
5 (26) T. Lopes, N. C. Mestre, S. Maria, T. Sabóia-morais and M. João, Environmental
6
7 behaviour and ecotoxicity of quantum dots at various trophic levels : A review, *Environ.*
8
9 *Int.*, 2017, **98**, 1–17.
- 10
11 (27) K-T. Yong, W.-C. Law, R. Hu, L. Ye, L. Liu, M. T. Swihart and P. N. Prasad,
12
13 Nanotoxicity assessment of quantum dots: From cellular to primate studies, *Chem. Soc.*
14
15 *Rev.*, 2013, **42**, 1236–1250.
- 16
17 (28) J. J. Wu, V. S. S. K. Kondeti, P. J. Bruggeman and U. R. Kortshagen, Luminescent ,
18
19 water-soluble silicon quantum dots via micro-plasma surface treatment, *J. Phys. D: Appl.*
20
21 *Phys.*, 2016, **49**, 08LT02.
- 22
23 (29) Y. Yiu, G. Fan, A. Fermi, R. Mazzaro, V. Morandi, P. Ceroni, D-M. Smilgies and B. A.
24
25 Korgel, Size-dependent photoluminescence efficiency of silicon nanocrystal quantum dots, *J.*
26
27 *Phys. Chem. C*, 2017, **121**, 23240-23248.
- 28
29
30
31
32
33
34
35 (30) M. Stan, C. Sima, L. O. Cinteza and A. Dinischiotu, Silicon-based quantum dots induce
36
37 inflammation in human lung cells and disrupt extracellular matrix homeostasis, *FEBS J.*,
38
39 2015, **282**, 2914–2929.
- 40
41 (31) L. Stanca, S. N. Petrache, A. I. Serban, A. C. Staicu, C. Sima, M. C. Munteanu, Z. Otilia,
42
43 D. Dinu and A. Dinischiotu, Interaction of silicon-based quantum dots with Gibel carp
44
45 liver : Oxidative and structural modifications, *Nanoscale Res. Lett.*, 2013, **8**, 254.
- 46
47 (32) J. T. Buchman, A. Rahnamoun, K. M. Landy, X. Zhang, A. M. Vartanian, L. M. Jacob, C.
48
49 J. Murphy, R. Hernandez and C.L. Haynes, Using an environmentally-relevant panel of Gram-
50
51
52
53
54
55
56
57
58
59
60

1
2
3 negative bacteria to assess the toxicity of polyallylamine hydrochloride-wrapped gold
4 nanoparticles, *Environ. Sci.: Nano*, 2018, **5**, 279-288.
5
6

7
8 (33) H. H. Hau, A. Gilbert, D. Coursolle and J. A. Gralnick, Mechanism and consequences of
9 anaerobic respiration of cobalt by *Shewanella oneidensis* strain MR-1, *Appl. Environ. Microbiol.*,
10 2008, **74**, 6880-6886.
11
12
13

14
15 (34) H. A. Wiatrowski, P. M. Ward and T. Barkay, Novel reduction of mercury(II) by
16 mercury-sensitive dissimilatory metal reducing bacteria, *Environ. Sci. Technol.*, 2006, **40**, 6690-
17 6696.
18
19
20
21

22
23 (35) S. Bencharit and M. J. Ward, Chemotactic responses to metals and anaerobic electron
24 acceptors in *Shewanella oneidensis* MR-1, *J. Bacteriol.*, 2005, **187**, 5049-5043.
25
26
27

28
29 (36) L. Ye, K.-T. Yong, L. Liu, I. Roy, R. Hu, J. Zhu, H. Cai, W.-C. Law, J. Liu, K. Wang, J.
30 Liu, Y. Liu, Y. Hu, X. Zhang, M. T. Swihart and P. N. Prasad, A pilot study in non-human
31 primates shows no adverse response to intravenous injection of quantum dots, *Nat. Nanotech.*,
32 2012, **7**, 453-458.
33
34
35
36

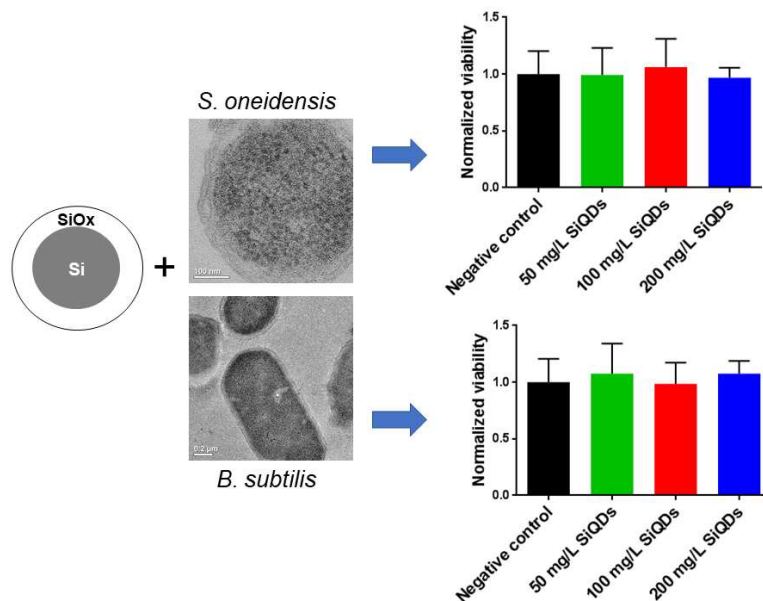
37
38 (37) J. Liu, F. Erogbogbo, K.-T. Yong, L. Ye, J. Liu, R. Hu, H. Chen, Y. Hu, Y. Yang, J. Yang,
39 I. Roy, N. A. Karker, M. T. Swihart and P. N. Prasad, **Assessing clinical prospects of silicon**
40 **quantum dots: Studies in mice and monkeys**, *ACS Nano*, 2013, **7**, 7303-7310.(38) R. J.
41 Anthony, D. J. Rowe, M. Stein, J. Yang and U. Kortshagen, Routes to achieving high quantum
42 yield luminescence from gas-phase-produced silicon nanocrystals, *Adv. Funct. Mater.*, 2011, **21**,
43 4042-4046.
44
45
46
47
48
49
50
51

52
53 (39) D. Hanaor, M. Michelazzi, C. Leonelli and C. C. Sorrell, The effects of carboxylic acids
54 on the aqueous dispersion and electrophoretic deposition of ZrO₂, *J. Eur. Ceram. Soc.*,
55
56
57

- 2012, **32**, 235–244.
- (40) L. Mangolini, D. Jurbergs, E. Rogojina and U. Kortshagen, Synthesis and characterization of strongly luminescing ZnS-capped CdSe nanocrystals, *J. Lumin.*, 2006, **121**, 327-334.
- (41) M. A. Hines and P. Guyot-sionnest, Photoluminescence intermittency from single quantum dots to organic molecules: Emerging themes, *J. Phys. Chem.*, 1996, **100**, 468–471.
- (42) A. M. Derfus, W. C. W. Chan and S. N. Bhatia, Probing the cytotoxicity of semiconductor quantum dots, *Nano Lett.*, 2004, **4**, 11-18.
- (43) J. H. Priester, P. K. Stoimenov, R. E. Mielke, S. M. Webb, C. Ehrhardt, J. I. N. P. Zhang, and G. D. Stucky, Effects of soluble cadmium salts versus CdSe quantum dots on the growth of planktonic *Pseudomonas aeruginosa*, *Environ. Sci. Technol.*, 2009, **43**, 2589–2594.
- (44) E. Yaghini, K. F. Pirker, C. W. M. Kay, A. M. Seifalian and A. J. Macrobert, Quantification of reactive oxygen species generation by photoexcitation of PEGylated quantum dots, *Small*, 2014, **10**, 5106–5115.
- (45) A. Nagy, A. Steinbru, J. Gao, N. Doggett, J. A. Hollingsworth and R. Iyer, Comprehensive analysis of the effects of CdSe quantum dot size , surface charge , and functionalization on primary human lung cells, *ACS Nano*, 2012, **6**, 4748–4762.
- (46) J. A. Imlay, The molecular mechanisms and physiological consequences of oxidative stress: lessons from a model bacterium, *Nat. Rev. Microbiol.* 2013, **11**, 443–454.
- (47) J. Yin and H. Gao, Stress responses of shewanella, *Int. J. Microbiol.*, 2011, **2011**, 863623.
- (48) A. Hartwig, M. Asmuss, I. Ehleben, U. Herzer, D. Kostelac, A. Pelzer, T. Schwerdtle and A. Bürkle, Interference by toxic metal ions with DNA repair processes and cell cycle control : Molecular mechanisms, *Environ Health Perspect.*, 2002, **110**, 797–799.

- 1
2
3 (49) K. Smeets, A. Cuypers, A. Lambrechts, B. Semane and P. Hoet, Induction of oxidative
4 stress and antioxidative mechanisms in *Phaseolus vulgaris* after Cd application, *Plant*
5
6 *Physiol Biochem.*, 2005, **43**, 437–444.
7
8
9
10 (50) D. H. Nies, Resistance to cadmium, cobalt, zinc, and nickel in microbes, *Plasmid*, 1992,
11
12 **28**, 17–28.
13
14 (51) Z. V. Feng, I. L. Gunsolus, T. A. Qiu, K. R. Hurley, L. H. Nyberg, H. Frew, K. P.
15
16 Johnson, A. M. Vartanian, L. M. Jacob, S. E. Lohse, M. D. Torelli, R. J. Hamers, C. J.
17
18 Murphy and C. L. Haynes, Impacts of gold nanoparticle charge and ligand type on surface
19
20 binding and toxicity to Gram-negative and Gram-positive bacteria, *Chem. Sci.*, 2015, **6**,
21
22 5186–5196.
23
24
25 (52) R. Schneider, C. Wolpert, H. Guilloteau, L. Balan, J. Lambert and C. Merlin, The
26
27 exposure of bacteria to CdTe-core quantum dots : The importance of surface chemistry on
28
29 cytotoxicity, *Nanotechnology*, 2009, **20**, 225101.
30
31
32 (53) O. Huismant, R. D'Ari and S. Gottesmant, Cell-division control in *Escherichia coli*:
33
34 Specific induction of the SOS function SfiA protein is sufficient to block septation, *Proc.*
35
36 *Natl. Acad. Sci. U S A.*, 1984, **81**, 4490-4494.
37
38
39 (54) M. Adjou, P. Tréguer, C. Dumousseaud, R. Corvaisier, M. A. Brzezinski and D. M.
40
41 Nelson, Particulate silica and Si recycling in the surface waters of the Eastern Equatorial
42
43 Pacific, *Deep-Sea Research II*, **58**, 449-461.
44
45
46 (55) C. Beucher, P. Tréguer, A.-M. Hapette, R. Corvaisier, N. Metzl and J.-J. Pichon, Intense
47
48 summer Si-recycling in the surface Southern Ocean, *Geophys. Res. Lett.*,
49
50 **31**,10.1029/2003GL018998.
51
52
53
54
55
56
57
58
59
60

Table of contents entry:



The investigated Si quantum dots do not affect the viability of bacterial cells, and could potentially prove to be a more environment-friendly, sustainable, and cheaper alternative to traditional Cd-based quantum dots.